DEUTSCHES ELEKTRONEN-SYNCHROTRON DESY

DESY SR-77/10
June 1977

Angle Resolved Photoemission from the NaCl (100)-face

by

F.-J. Himpsel, W. Steinmann

Sektion Physik der Universität München

NOTKESTRASSE 85 · 2 HAMBURG 52

To be sure that your preprints are promptly included in the
HIGH ENERGY PHYSICS INDEX ,
send them to the following address (if possible by air mail) :

DESY
Bibliothek
Notkestraße 85
2 Hamburg 52
Germany

Angle Resolved Photoemission from the NaCl (100)-face[+]

F.-J. Himpsel[*], W. Steinmann;
Sektion Physik der Universität München, München, Germany

Abstract

The angle and energy distribution of photoelectrons from the (100)-face of NaCl single crystals were measured for photon energies ranging from 15 eV to 30 eV by use of synchrotron radiation. Critical points of the band structure along the line ΓΔX of the Brillouin zone were derived from the data. The energies measured from the top of the valence band in eV are the following:

X_4' = -2,4 ± 0,2; X_5' = -1,4 ± 0,2; X_1 = 11,4 ± 0,5; X_3 = 12,0 ± 0,5;
X_4' = 17,0 ± 0,5; Γ_{25}' = 17,2 ± 0,2;
and a minimum of the third conduction band on Δ_1 at 13,7±0,5.
The assignment for X_5 (21 eV) and Γ_{12} (18,7 eV) is less certain. The evaluation is facilitated by the fact that many of the Bloch states on the ΓΔX-line do not contribute to the photoemission in the (100)-direction since they do not contain the appropriate plane wave components.

[+]Work supported by Deutsches Elektronen Synchrotron DESY, Hamburg

[*]Present address: IBM Thomas J. Watson Research Center
Yorktown Heights, New York 10598

1. Introduction

Angle resolved photoemission results from metals and semiconductors have been explained fairly successfully by the volume band structure of these materials. For insulators both the experimental situation and the status of the theory have not progressed as far. Photoemission from bulk insulators leads to charging which has to be compensated. Calculations suffer from the fact, that the bands are far from being free electron like and that correlation effects (like the polarization of the surrounding of an electron or hole) have to be included. Therefore calculations by various methods diverge not only in their energy scale but also in the sequence of certain conduction bands.

Angle resolved experiments on insulators have started with alkali halides[1]. It has been shown that the angular distribution below the electron electron scattering threshold is determined only by the conduction bands because of multiple electron phonon scattering. Above threshold the direct transition model starts to become valid as in the case of metals and semiconductors. Thus the problem of finding the correct conduction bands can be separated from the determination of the valence bands. Another advantage of insulators is the large escape depth of the photoelectrons in the order of several hundred Angstroms below the threshold for electron electron scattering. This guarantees that surface effects play a minor role, and the experimental results can essentially be accounted for by the volume band structure. In this paper we present angle resolved photoemission data from NaCl (100)-faces which cover a wide range of angles and energies. These experimental results contain information on the band structure in the whole Brillouin zone. We evaluate only the part of it pertinent to the ΓΔX line which is most easily accessible and straightforward in the assignment.

2. Experimental

Experiments were performed at the DESY electron synchrotron with a 1m-normal incidence monochromator. The sample chamber is scetched in fig. 1. It contains a fixed electron energy analyzer of the filter lens type with a resolution of 0,2 eV and an acceptance cone of 3^{o} full aperture. The escape angle of the photoelectrons with respect to the crystal axes is varied by turning the sample. The vacuum was

in the 10^{-10} Torr range. The samples could be cleaved in situ if the polar escape angle was fixed. In this case the samples were mounted on a rotary feedthrough which could be attached in three different positions to the vacuum chamber such that the polar angle θ (measured from the normal of the sample surface) was 0^{o}, 45^{o}, and 72^{o} respectively. The results shown in fig. 2 and 8 were taken in this experimental arrangement. If the polar angle had to be varied during the measurement a manipulator with two rotations (full range for θ and 180^{o} range for the azimuth ϕ) was applied. In this case, however, the samples could not be cleaved in the sample chamber. The surfaces prepared outside showed a reduced contrast of the angular distribution as compared to the samples cleaved in situ but the structures remained. This is understandable in view of the result of Estel et al.[2] who found that H_2O desorbs almost completely from an air cleaved NaCl (100)-face below 10^{-8} Torr. Upon heating, however, a permanent hydroxide layer is formed. Therefore we did not bake out the sample chamber with air cleaved samples. The base pressure, in this case, was in the 10^{-9} Torr range. The results shown in fig. 5 and 7 were obtained in this configuration.

The charging of the samples was compensated by a cloud of low energy electrons produced by a heated filament, which was outside the magnetic shielding of the drift space (see ref. 1). The sample potential was stabilized to ±0,3 eV by this method.

3. Results and Discussion

3.1 Energy Distributions for Escape Normal to the (100)-Face

3.11 General Remarks

Energy distributions (EDCs) for electrons escaping normal to the (100)-surface are displayed in fig. 2 for different photon energies $\hbar\omega$. The final energy of the electrons with respect to the top of the valence band, E_f, was determined from the high energy edge of the EDC and the photon energy. The electron electron scattering threshold is at E_f = 16.5 eV as can be seen from the minimum energy loss of 7,5 eV in fig. 2 and the energy gap value of 9.0 eV given in ref. 3. At threshold the energy lost in the scattering process is used to create an exciton. Among the final states in the conduction band only those with $\vec{K}$-vectors

on the line $\Gamma\Delta X$ can contribute to the photoemission in the direction of the surface normal (see fig. 6). This holds because the reduced wavevector component parallel to the surface is conserved during emission. It can be shown (see appendix) that only bands with Δ_1-symmetry have the proper angular characteristic to emit in the (100)-direction. At the points Γ and X the photoemission vanishes because the group velocity goes to zero. - As a starting point we use the band structure calculation[5] shown in fig. 3. The bands derived from our data are shown in fig. 4.

3.12 Interpretation in Terms of the Band Structure

The EDCs at $\hbar\omega$ = 28 eV and 31 eV originate from electrons which have undergone one or more electron electron scattering processes and additional multiple electron phonon scattering. They have lost the information about the energy and the wave-vector at the optical excitation - hence the EDC does not depend on the photon energy - and they are distributed rather uniformly over the conduction bands. Therefore we expect that these EDC's reflect the density of states of the Δ_1 conduction bands. The intensity rise below E_f = 11,4 eV is attributed to electrons from the first conduction band which has symmetry Δ_1. The next band is of Δ_2'-symmetry and does not contribute to the photoemission in (100)-direction. This results in a region of low intensity which extends up to E_f = 13,7 eV. There the third band starts, which has again Δ_1-symmetry. Band structure calculations indicate (see table) that the maximum of the first band is X_1 and the minimum of the third band on the Δ-axis lies inside the Brillouin zone. The strongest contribution from the third band is observed around E_f = 15 eV which is about 1 eV higher than the minimum.

Above the electron electron scattering threshold there is a pinning of the peak of the EDCs to a final energy of 17,2 eV for photon energies between 18,5 and 20,0 eV. This indicates transitions from a valence band with strong dispersion (at least 1,5 eV) into a conduction band which is flat compared to this valence band. A similar but less pronounced structure is observed at E_f = 18,7 eV. We attribute the maximum at E_f = 17,2 eV to transitions from the lower valence band into final states around Γ_{25}' (e.g. $\Lambda_1 \rightarrow \Delta_5$). The structure at 18,7 eV may correspond to a similar transition into final states around Γ_{12}. Two remarks should be made concerning this interpretation:

1) The conduction bands Δ_5 and Δ_2 cannot contribute directly to the emission into the (001)-direction for symmetry reasons (see appendix). However, Δ_5 states near Γ'_{25} can be transformed into Δ_1-states by electron phonon scattering without detectable change in energy. Electron phonon scattering still occurs around E_f = 17 eV. This can be seen from the fact that the angular distribution does not depend on the initial state energy (see ref. 1). Indeed, for the flat part of the Δ_5-band we expect a relatively small electron phonon scattering length, because the group velocity is small. Typical electron phonon scattering lengths[9] are well below the electron electron scattering length of 80 Å derived from our data[10] for E_f = 17,2 eV. On the other hand, an electron which arrives in the Δ_1-bands has a much higher group velocity and may escape without further phonon scattering. For the Δ_2-band such an explanation is not possible, because the electron electron scattering length is too small (about 8 Å at E_f = 18,7 eV). Only the Δ_1-band connected to the point Γ_{12} contributes to the photoemission in direction to the surface normal.

2) The strong decrease of the emission intensity above the electron electron scattering threshold modulates the shape of the EDCs. It could be argued that this modulation is responsible for the main peak remaining constant for 18,5 eV < E_f < 20,0 eV. However, this would not be compatible with our observation that the EDCs behave differently in other escape directions.

For photon energies above 20 eV the EDC consists of two maxima which move to higher energies as the photon energy is increased such that $E_i = E_f - \hbar\omega$ remains constant. Therefore they are interpreted as maxima in the density of the initial states at the points X'_5 and X'_4. In this range of final energies, all states of Δ_1-symmetry must be evanescent according to the calculation in ref. 5. Indeed, we observe such a low photoemission intensity that the corresponding escape depth is less than 4 Å. We obtain -2.4 eV for the initial energy of X'_4 and -1.4 eV for X'_5.

3.2 Angular Distribution of the Intensity

Fig. 5 shows energy distributions of electrons produced by electron electron scattering from highly excited primaries. The escape direction is varied in the two symmetry planes (010) and ($\bar{1}$10). Like the curves shown in the lower part of fig. 2 ($\hbar\omega$ = 28 eV, 30 eV) these EDCs are insensitive to the photon energy and can be interpreted using only the conduction bands. The insert compares an angle integrated EDC from an evaporated film with the angle resolved data. The two peaks C and D appear for different escape directions, C at high polar angles in the (010)-plane, D for escape normal to the (001) surface. F coincides with the onset of electron electron scattering. Peak D is the same as the one shown in the lower part of fig. 2 and corresponds to the minimum of the third conduction band on the Δ-axis. To account for maximum C one has first to determine which part of the Brillouin zone can contribute to the emission in this range of energy and escape angle. The component of $\vec{K}_v$ parallel to the surface (see fig. 6) can be calculated from the measured energy and escape direction by the relation

$$(1a) \qquad |\vec{K}''_v| = \sqrt{(2\,m/\hbar^2)\cdot(E - E_v)}\sin\theta$$

which for NaCl takes the form

$$(1b) \qquad |\vec{K}''_v|/(2\pi/a) = 0{,}459\sqrt{(E - E_v)/eV}\,\sin\theta$$

E_v is the vacuum level, θ the angle between the escape direction and the surface normal. With E_f = 13 eV, E_v = 9 eV[2], θ = 65° equ. 1b yields $|\vec{K}''_v|/(2\pi/a)$ = 0,83. The possible $\vec{K}$-values of the contributing Bloch states are shown as dotted lines in fig. 6.

The band structure in fig. 3 shows a minimum in this E, $\vec{K}$-range at X_3, which is the lowest point of the second band. This state cannot be observed in photoemission since the electron waves are totally reflected at an energy of 4 eV above the vacuum level. This can be seen by setting the left side of equ. 1b equal to unity. At θ = 65°, regions of the $\vec{K}$-space close to X_3, but with smaller $\vec{K}''$, contribute to peak C. Their energy is certainly higher than the minimum. If we assume, as in the case of the minimum of the Δ_1-band discussed above, that the peak occurs about 1 eV above the lowest point, we obtain an estimate of 12 eV for the energy value of X_3. Hence, by studying the EDC at oblique escape angles we have found the piece of the band structure on the Δ-axis which was missing in the emission normal to the (100)-face.

The angular distribution of the photoemission intensity at fixed final energy (E_f = 15,7 eV) is represented in fig. 7 by lines of equal intensity. The azimuth ϕ is related to the component of the $\vec{K}_v$-vector parallel to the surface, $\vec{K}_v''$; ϕ = (10) means that $\vec{K}_v''$ has a direction equivalent to the (10)-direction. There is low intensity in the (11)-escape planes. Bright spots are at $\theta = 55^o$, ϕ = (10) called peak A- and at $\theta = 65^o$, ϕ = (11) $\pm 10^o$ -peak B. Equ. 1b yields for A: $|\vec{K}_v''|/(2\pi/a) = 0{,}97$, which is practically on the surface of the Brillouin zone. It follows from fig. 6 that A originates from the line XZW in $\vec{K}$-space. For the general behaviour of the band structure we use again the calculation[5] shown in fig. 3. The final energy E_f = 15,7 eV is in the range of the fourth conduction band $X_5Z_2W_1'$. The corresponding Bloch states, however, do not contribute to the photoemission in the (10)-escape plane due to their angular characteristic as is shown in the appendix. Consequently peak A must originate from the third or fifth conduction band which have symmetry Z_3. The top of the third band is point X_4', the bottom of the fifth band is X_5. Thus we expect peak A to disappear in a certain energy range corresponding to the energy gap between the third and fifth band on the Z-axis. The dependence of the intensity of peak A on the final energy will show whether E_f = 15,7 eV lies in the third or fifth conduction band. Fig. 8 shows an azimuthal intensity distribution with E_f as parameter. The data were taken at a polar angle θ of 45^o which, according to equ. 1b, corresponds approximately to the boundary of the Brillouin zone ($|\vec{K}''| = 2\pi/a$) in the energy range in question. The maximum in the (10)-direction in fig. 8 corresponds to peak A in fig. 7. This maximum occurs at all final energies except in the range 17 eV < E_f < 21 eV. The boundaries of this energy gap correspond to the points X_4' and X_5 in the band structure. In some calculations this point has symmetry X_5'. In this case transitions from the valence bands are forbidden in contrast to the rather strong transition which we observe.

All obtained energy values of critical points are collected in the table and compared to more recent band structure calculations. To eliminate the rather high uncertainty of the calculations concerning the band gap energy we have related our results for the conduction bands to the bottom of the conduction band using the experimental band gap value given in ref. 3.

4. Conclusion

We have shown in this paper that angle resolved photoemission data can be used to determine critical points of threedimensional valence and conduction bands. This is achieved without detailed calculation using only qualitative preknowledge of the bands in symmetry directions and taking into account the angular characteristic of the wavefunction. The key information is given by the dependence of the observed structures on photon energy. This shows the advantage of synchrotron radiation as a light source for such experiments. Comparing our results with band structure calculations it appears that Hartree Fock calculations including polarization corrections give the best values for the energies of the critical points. An empirical pseudopotential calculation[4] agrees poorly with our data. It should be possible, however, to obtain improved pseudopotential parameters from our results. With such a pseudopotential it is rather straightforward to calculate the angular distribution of the photoemission for all escape angles (see ref. 10, 13). The result could be compared with the experimental data shown in fig. 7. This would be a test if the pseudopotential yields the correct conduction bands in the whole Brillouin zone. The improved band structure may be used to calculate optical absorption spectra. Comparison with experimental results could show, whether or not excitations into high conduction band states are influenced by excitonic effects.

Appendix: Contribution of Bloch States to a Given Escape Direction

The reduced wavevector parallel to the surface, $\vec{k}$, is a good quantum number if the crystal surface is periodic. For a Bloch state with reduced wavevector $\vec{k}$ which couples to the detected plane wave of wave vector $\vec{k}_v$ the conservation of $\vec{k}$ leads to the following relation:

$$(2) \qquad \vec{k}_{=} = \vec{k}_v'' + \vec{g}$$

" denotes the component parallel to the surface and $\vec{g}$ is a vector of the reciprocal surface lattice. The NaCl lattice is a fcc lattice with basis a/2 (111) (a = side length of the cube = 5,63 Å for NaCl). The reciprocal lattice of the (001)-surface is simple cubic with the basis vectors (11) and ($\bar{1}$1) (in units of $2\pi/a$), if we assume that there is no superstructure (see LEED-data in ref. 14). The coupling condition 2 is visualized in fig. 6. For a given wavevector $\vec{k}_v$ in the vacuum the

reduced $\vec{K}$-vectors of the Bloch states coupling to K_v are given by the intersection of at most two nonequivalent lines in the Brillouin zone with the energy surface. These lines can be constructed in the following way: Applying successively surface lattice vectors of the star (20) (in units of $2\pi/a$) to the rod $\vec{K}'' = \vec{K}''_v$ one obtains a rod in the square $|K_x| \leq 2\pi/a$, $|K_y| \leq 2\pi/a$ which contains the projection of the first Brillouin zone (of the volume lattice) onto the surface. Starting with this rod one obtains a second one in the same $\vec{K}''$-area using a surface lattice vector of the star (11). The symmetry properties of the point group have an effect on the angular distribution of the emitted electrons. We consider two examples for the discussion of the experimental results:

1) Escape direction normal to the (001)-surface.
The reduced wavevector parallel to the surface, $\vec{k}$, is zero in this case. We have the full symmetry group of the reciprocal surface lattice 4 mm (C_{4v} in Schoenflies notation). The only representation that yields an outgoing wave of the type $\exp(iK_z z)$ is Δ_1 (A_1 in Mulliken notation). (We neglect spin orbit coupling which is about 0,1 eV for the valence band of NaCl[3].) A Δ_2-type wave function $\psi(x,y,z)$ vanishes on the z-axis because the sign of ψ changes if x and y are interchanged. (Taking $\psi(x,y,z) = -\psi(y,x,z)$ and setting x=y=0 one obtains the relation $\psi(0,0,z) = -\psi(0,0,z)$ which results in $\psi(0,0,z) = 0$.) Hence a Δ_2-type Bloch function does not contribute to the photoemission normal to the (001)-surface as it has no partial wave with vanishing component parallel to the surface. A similar proof is possible for the remaining representations Δ_2', Δ_1', Δ_5 because they are odd either with respect to x or y.

2) Electron emission in the (010)-plane (ϕ = (10)) from Bloch states at the boundary of the Brillouin zone.
In this case E and θ have to be such that $|\vec{k}|/(2\pi/a) = 1$. From fig. 6 we see that the four equivalent points $\vec{k}$ = (10), (01), $(\bar{1}0)$, $(0\bar{1})$ of the surface Brillouin zone contribute. These points correspond to four rods in the reciprocal volume lattice which comprise the lines WZXZW along the z-direction of the volume Brillouin zone. The symmetry of the Bloch states on the Z-line is mm2 (C_{2v}). The states of the four rods have to be combined to form the total wavefunction which has the symmetry 4mm of the reduced wavevector parallel to the surface. If the

total wavefunction is an odd function of y, it will vanish on the xz-plane which is the plane of observation. Therefore, no contribution is expected from such states. The symmetry of the total wavefunction depends on the symmetry of the Z-type Bloch functions of the four rods which have to be combined. Three cases can be distinguished:

a) For Z_1-symmetry, the Bloch function is even with respect to both x and y. In this case, the total wave function will also be an even function of y. Hence Z_1 states will contribute to the observed photoemission.
b) For Z_3- and Z_4-symmetry, the Bloch functions are even with respect to x and odd with respect to y or vice versa. A Bloch function which is an even function of x and an odd function of y in the rod $\vec{K}''$ = (10), is odd with respect to x and even with respect to y in the rod $\vec{K}''$ = (01). Hence a linear combination of the four rods leads to a total wavefunction which is not necessarily odd with respect to y. Consequently, Z_3- and Z_4-states can contribute to the observed photoemission in general.
c) For Z_2-symmetry, the Bloch functions are odd functions of both x and y. A linear combination of the four rods will also lead to an odd function of y. Z_2-states will therefore not contribute to the photoemission in the xz-plane.

References

1 F.J. Himpsel, W. Steinmann, Phys. Rev. Lett 35, 1025 (1975)

2 J. Estel, H. Hoinkes, H. Kaarmann, N. Nahr, H. Wilsch, Surf. Siece 54, 393 (1976)

3 D.M. Roessler, W.C. Walker, Phys. Rev. 166, 599 (1968)

4 C.Y. Fong, M.L. Cohen, Phys. Rev. 185, 1168 (1969)

5 J.L. Page, E.H. Hygh, Phys. Rev. B1, 3472 (1970)

6 N.O. Lipari, A.B. Kunz, Phys. Rev. B3, 491 (1971)

7 F. Perrot, phys. stat. sol. (b) 52, 163 (1972)

8 J.S. Melvin, T. Smith, phys. stat. sol. (b) 49, 173 (1972)

9 J. Llacer, E.L. Garwin, J. Appl. Phys. 40, 2766 (1969)

10 F.J. Himpsel, thesis, München 1976, unpublished

11 A.D. Baer, G.J. Lapeyre, Phys. Rev. Lett. 31 304 (1973)

12 G.J. Lapeyre, J. Anderson, J.A. Knapp, P.L. Gobby in
"Vacuum Ultraviolett Radiation Physics"
ed. by E.E. Koch, R. Haensel, C. Kunz
(Vieweg/Pergamon, Braunschweig 1974), p. 380

13 F.J. Himpsel, W. Steinmann in
"Photoemission", Proceedings of an International Symposium
Noordwijk, Netherlands, ESA SP 118 REV.1, Nov. 1976, p. 137

14 J. Bandet, L. Touzillier, A. Malavaud, Y. Quemener, Surf. Sci. 51,
174 (1975)

Table: NaCl Band Structure Data

	Calculations (since 1969)					Experiment
Reference	4	5	6	7	8	3
Method	EPM	APW	HF	HF	APW	Opt. Refl.
$E_g=\Gamma_1-\Gamma_{15}$	(9,0)*	(8,8)*	10,0	8,4	5,0	9,0
Initial states, measured from the top of the valence band (Γ_{15})						This work**
$X_5'-\Gamma_{15}$	-0,2	-0,2	-1,3	-0,6	-0,5	-1,4±0,2
$X_4'-\Gamma_{15}$	-1,0	-0,6	-3,8	-1,5	-1,7	-2,4±0,2
Final states, measured from the bottom of the conduction band (Γ_1)						
$\Gamma_n, X_n-\Gamma_1$						
X_1	1,0	3,1	2,9	3,4	3,4	2,4±0,5
X_3	1,0	4,0	3,0	2,0	2,6	3,0±0,5
Minimum Λ_1	3,6	5,0	6,0		5,2	4,7±0,5
X_4'	8,8	5,2	7,4	5,2	5,7	$8,0\pm^{0,5}_{1,0}$
X_5	7,3	9,0	11,3 (X_5')	10,3 (X_5')		12,0
Γ_{25}'	3,7	6,9	7,6	5,6	6,0	8,2±0,2
Γ_{12}	4,2	8,4	10,0	8,1		9,7

All energies in eV

*Values fitted to experimental data

**The energies are measured from the top of the valence band.
For the conduction bands E_g = 9,0 eV has been subtracted.

Figure captions

Fig. 1 Schematic drawing of the experimental arrangement. FIL = hot filament for charging compensation, SP = exit slit of the monochromator, EEA = electron energy analyzer. The electric field vector lies in the plane of the figure.

Fig. 2 EDCs of photoelectrons escaping normal to the (100)-face of NaCl. The zero line is shifted proportional to the photon energy $\hbar\omega$. E_f is the energy measured from the top of the valence band. The EDCs are normalized to equal area except the EDCs for $\hbar\omega$ = 28 eV and 30 eV where the intensity per incident photon is shown.

Fig. 3 Band structure of NaCl after Page and Hygh (ref. 5)

Fig. 4 Model band structure of NaCl obtained from the experimental results of this work (dots) in combination with recent calculations (ref. 5 and 6). Energies are measured from the top of the valence band (Γ_{15}).

Fig. 5 EDCs of secondaries produced by electron electron scattering for different escape directions. The insert is taken from ref. 12. Compared to ref. 12 our EDCs are shifted by 0,5 eV to higher energy because we use a different method to determine the upper edge of the EDCs.

Fig. 6 Correlation between the wavevector of a plane wave in the vacuum, $\vec{K}_v$, and the wavevectors of Bloch states that can contribute to the emission in the direction of $\vec{K}_v$ (dots). Shown are top and side view of the Brillouin zones for a fcc lattice and the twodimensional Brillouin zone of the (001)-surface (dashed). A detailed explanation is given in the appendix.

Fig. 7 Angular distribution of the photoelectron intensity from a NaCl (001)-face for a photon energy $\hbar\omega$ = 17 eV and electron energy E_f = 15,7 eV (measured from the top of the valence band). The polar angle θ and the azimuth φ are represented in stereographic projection. (10) and (11) mark a φ corresponding to the (100) and (110) escape planes respectively (or equivalent planes). Heavy lines denote intensity maxima thin lines minima.

Fig. 8 Azimuthal pattern of the valence band photoemission from the NaCl (001)-face. The zero line is shifted proportional to the final state energy E_f as indicated on the right hand side of the figure. $E_i = E_f - \hbar\omega$. The curves are normalized with respect to their maximum value (from ref. 1).

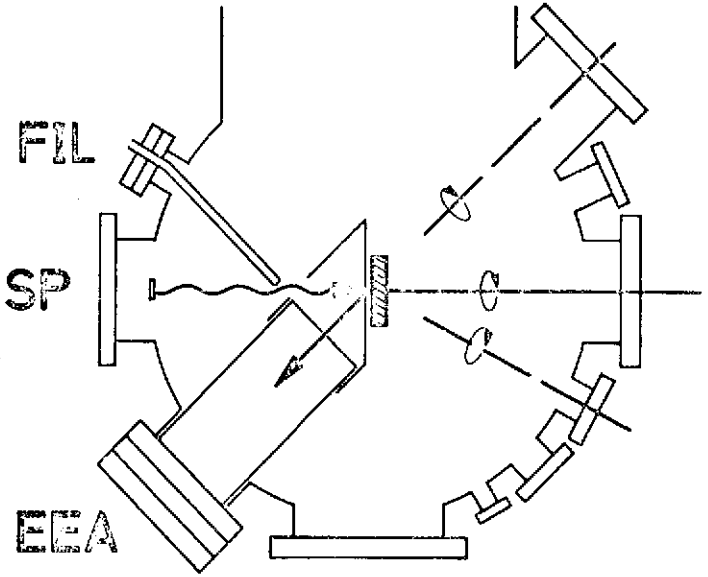
FIL
SP
EEA

Fig. 1

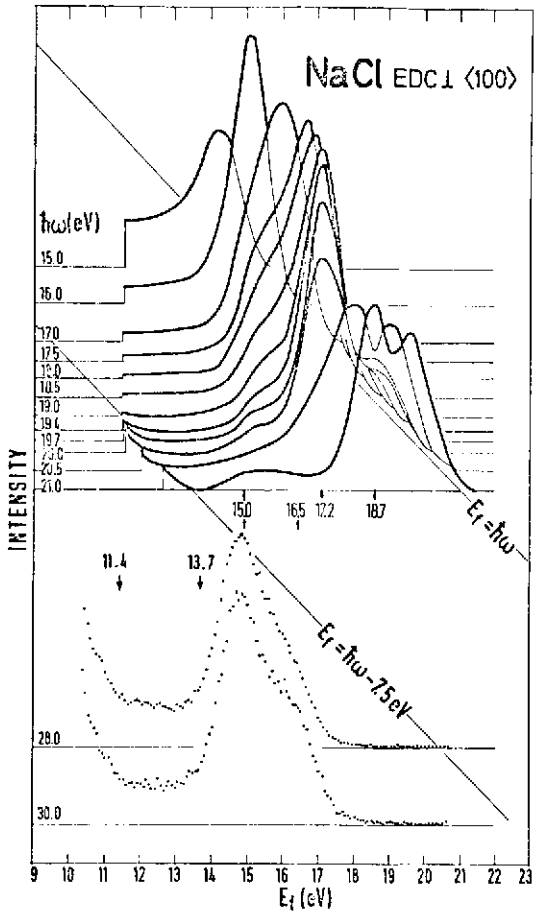
NaCl EDC ⊥ ⟨100⟩
ħω(eV)
15.0
16.0
17.0
17.5
18.0
18.5
19.0
19.4
19.7
20.0
20.5
21.0
15.0
16.5
17.2
18.7
$E_f = \hbar\omega$
11.4
13.7
$E_f = \hbar\omega - 7.5eV$
28.0
30.0
INTENSITY
9 10 11 12 13 14 15 16 17 18 19 20 21 22 23
E_f (eV)

Fig. 2

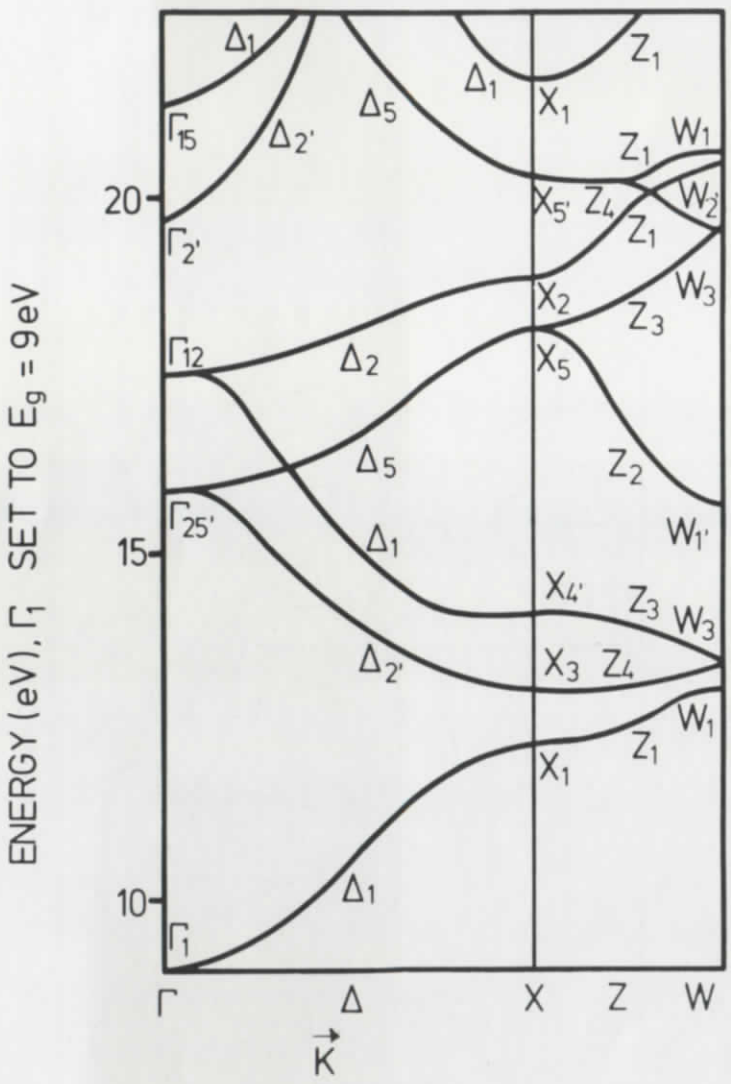
ENERGY (eV), Γ1 SET TO Eg = 9eV
20
15
10
Γ
Δ
X
Z
W
K
Γ15
Δ1
Δ2'
Δ5
X1
Z1
W1
X5'
Z4
W2
Γ2'
X2
W3
Z3
Γ12
Δ2
X5
Z2
Γ25'
W1'
X4'
X3
Γ1

Fig. 3

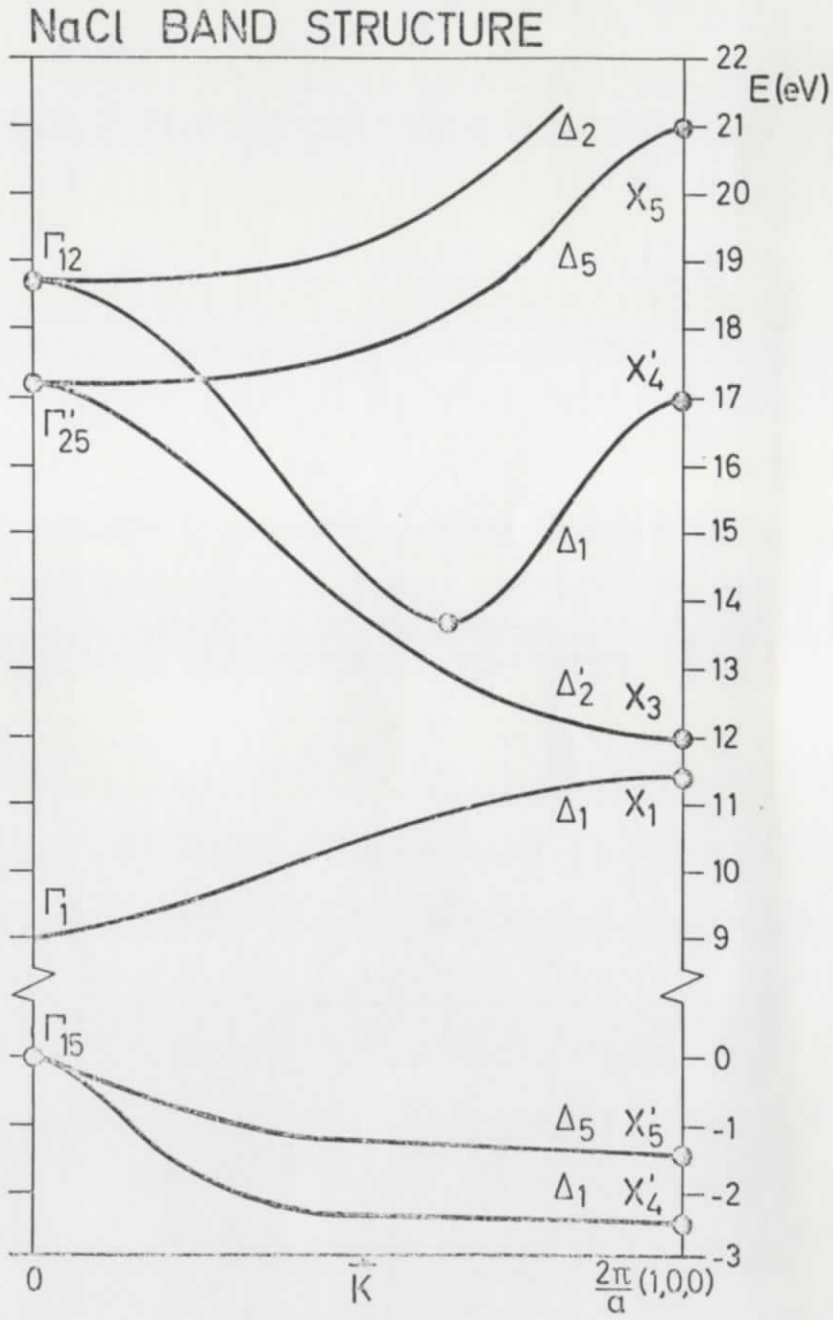
NaCl BAND STRUCTURE
E(eV)
22
21
20
19
18
17
16
15
14
13
12
11
10
9
0
-1
-2
-3
Δ2
X5
Γ12
Δ5
X'4
Γ'25
Δ1
Δ'2
X3
Δ1
X1
Γ1
Γ15
Δ5
X'5
Δ1
X'4
0
K
2π/a (1,0,0)

Fig. 4

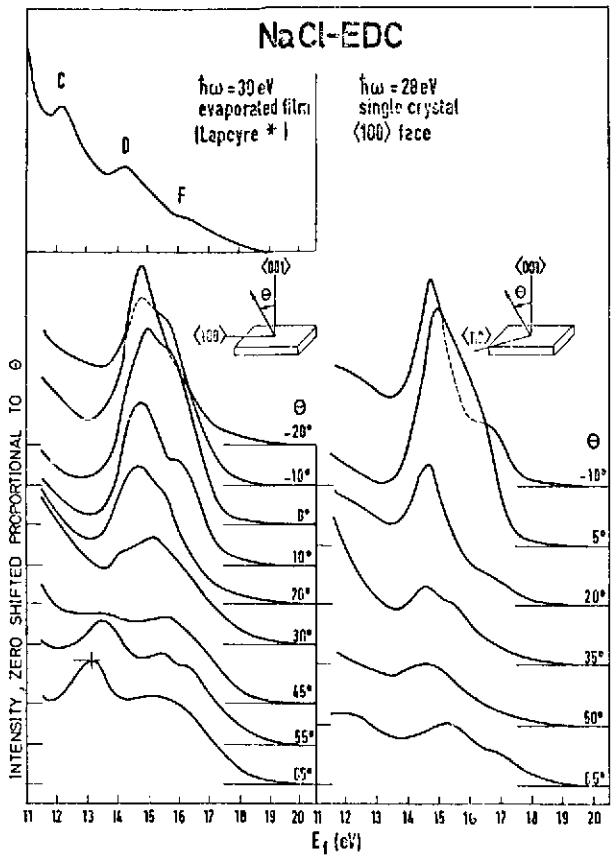
NaCl-EDC
ħω = 39 eV
evaporated film
(Lapeyre *)
ħω = 28 eV
single crystal
⟨100⟩ face
C
D
F
⟨001⟩
Θ
⟨100⟩
⟨110⟩
-20°
-10°
0°
10°
20°
30°
45°
55°
65°
5°
35°
60°
INTENSITY, ZERO SHIFTED PROPORTIONAL TO Θ
11 12 13 14 15 16 17 18 19 20
E_f (eV)

Fig. 5

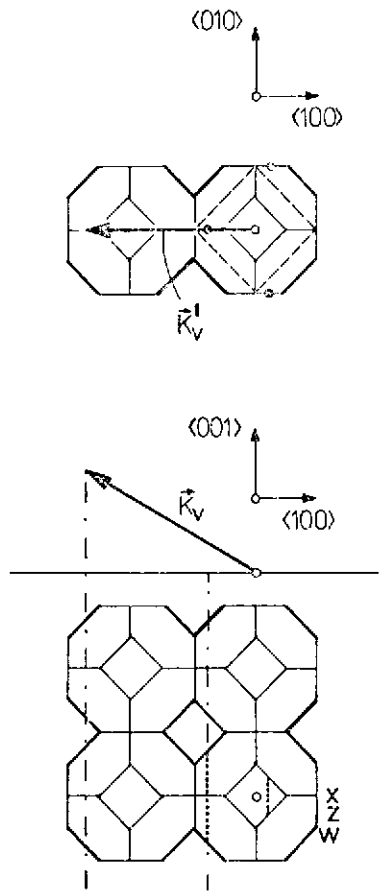
⟨010⟩
⟨100⟩
$\vec{K}_v'$
⟨001⟩
$\vec{K}_v$
⟨100⟩
X
Z
W

Fig. 6

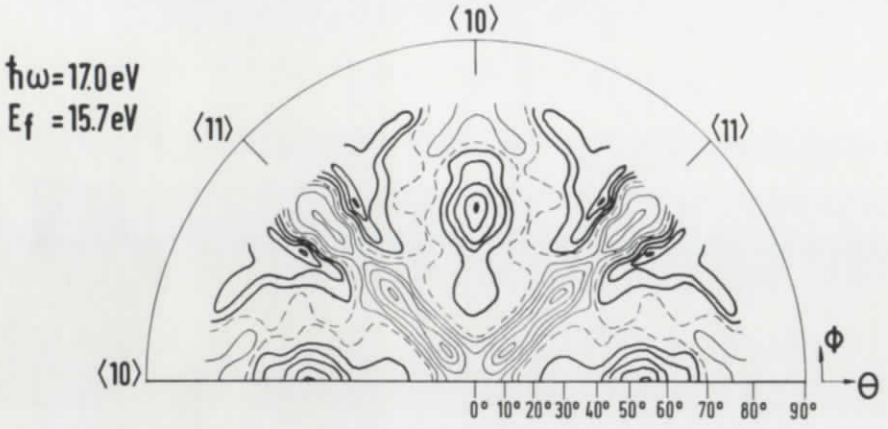
ħω=17.0eV
E_f =15.7eV
⟨10⟩
⟨11⟩
⟨11⟩
⟨10⟩
0° 10° 20° 30° 40° 50° 60° 70° 80° 90°
Φ
Θ

Fig. 7

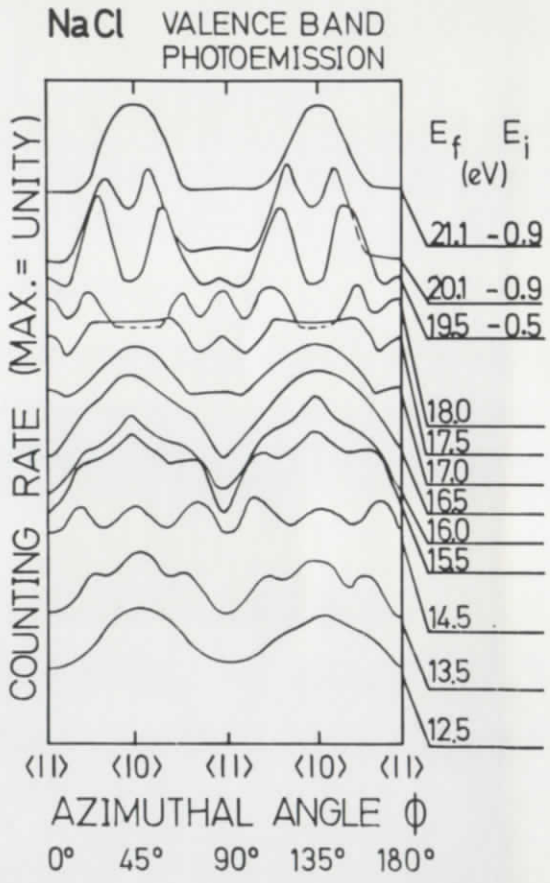
NaCl VALENCE BAND PHOTOEMISSION
COUNTING RATE (MAX.= UNITY)
E_f E_i (eV)
21.1 -0.9
20.1 -0.9
19.5 -0.5
18.0
17.5
17.0
16.5
16.0
15.5
14.5
13.5
12.5
⟨11⟩ ⟨10⟩ ⟨11⟩ ⟨10⟩ ⟨11⟩
AZIMUTHAL ANGLE Φ
0° 45° 90° 135° 180°

Fig. 8